

## Structure of stepped surfaces: Cu{320}

Y. Tian, J. Quinn, K.-W. Lin, and F. Jona

*Department of Materials Science and Engineering, State University of New York, Stony Brook, New York 11794-2275*

(Received 20 September 1999)

After a brief discussion of the problems involved in the determination of the structure of stepped surfaces, we report the results of a quantitative low-energy electron diffraction (QLEED) analysis of a Cu{320} surface. This surface features {110} terraces with three atom rows, separated by steps whose normal lies in the  $\langle 001 \rangle$  direction. The distance between successive {320} layers in the bulk is  $0.501 \text{ \AA}$ —one of the shortest interlayer distances studied to date. The analysis was done with the CHANGE computer program on a desktop computer. Calling  $\Delta d_{ij}$  the change in the distance between layers  $i$  and  $j$ , we found the following multilayer sequence:  $\Delta d_{12} = (-24 \pm 6)\%$ ,  $\Delta d_{23} = (-16 \pm 12)\%$ , and  $\Delta d_{34} = (+10 \pm 6)\%$ . The problems involved in the collection of experimental data and in the QLEED analysis of stepped surfaces are discussed.

### I. INTRODUCTION

Atomic steps play important roles on *real* crystal surfaces, even on those that are usually labeled flat or low index. This is because atoms at step edges can be dislodged more easily than other surface atoms and also serve as nucleation centers, thus affecting morphology, energetics, and reactivity of surfaces. Catalysis, crystal growth, oxidation, corrosion are all phenomena that are affected by surface steps.

For many of these reasons, much attention has been and is being devoted to the study of steps and their effects on a variety of surface properties, e.g., roughening, melting, vibrations, multilayer relaxations, etc. Most of these studies are theoretical, with relatively few experimental confirmations.

The most convenient object to consider for experimental studies of steps is a so-called stepped surface. A stepped surface is obtained by cutting a low-Miller-index surface (such as {001}, {110}, or {111}) at a small angle to the surface normal. The result is a surface with a periodic sequence of monatomic or diatomic steps separated by low-Miller-index terraces, the width of the latter being larger, the smaller the angle of cut. The atoms at the upper step edges lie mostly on a high-Miller-index plane, which is the first layer of the inclined high-index surface. The atomic planes parallel to this surface are separated by distances that are smaller, the smaller the angle of cut.

High-index surfaces generally exhibit large multilayer relaxations, proportionally much larger than their low-index counterparts. Study of this multilayer relaxation reveals the relative positions of the step-edge atoms and all atoms in the terraces. For this reason, most investigations of stepped surfaces focus on determining and understanding their multilayer relaxations.

The literature in this field is rich: we mention here only some of the most recent works.<sup>1-5</sup> The majority of the studies concern stepped surfaces of face-centered-cubic metals, particularly Al and Cu, and predominantly surfaces of the type  $\{11(2n+1)\}$ ,  $n=1,2,3,\dots$ .<sup>1-4</sup> On these surfaces, each terrace contains  $n+1$  rows of atoms, corresponding to as many layers, and the first  $n$  layers are predicted to exhibit *inward* relaxations (i.e., contractions), while the final  $n+1$ st layer has *outward* relaxation (expansion). This se-

quence is periodic, with period equal to the number of atom rows in each terrace. Hence, denoting a contraction by the  $-$  sign and an expansion by a  $+$  sign, the sequence, e.g., for fcc{113} is  $(- + \dots)$ , for fcc {115} is  $(- - + \dots)$ , for fcc {117} is  $(- - - + \dots)$ , etc. On most of these surfaces, parallel relaxations of the top layers are also predicted.

Only in very few cases have these theoretical predictions been confirmed by experiments, because experimental studies of multilayer relaxations on stepped surfaces are rather rare. The reason is that most such surfaces have small interlayer spacings, small meaning less than  $1 \text{ \AA}$ . The most successful experimental technique for the determination of multilayer relaxations of crystal surfaces is quantitative low-energy electron diffraction (QLEED), but this technique encounters problems when the bulk interlayer spacing becomes significantly smaller than  $1 \text{ \AA}$  as we explain presently.

Most of the computer programs used in QLEED analyses use a plane-wave expansion to represent the wave function between atomic layers. The diffracted beams in QLEED are special plane waves that have constant energy, and higher members of the plane-wave (beam) expansion exhibit increasing attenuation in the direction perpendicular to the surface. When the distance between atomic layers becomes small, more beams should be included in the expansion. However, in practice the beam expansion is limited to a finite number of beams—a result of computational limitations. When the bulk interlayer spacing ( $d_{\text{bulk}}$ ) becomes substantially smaller than  $1 \text{ \AA}$ , this limit is exceeded, and the calculation fails to converge. Hence, most computer programs cannot be used to analyze surfaces with  $d_{\text{bulk}} \ll 1 \text{ \AA}$ .

Presently, there are only two solutions to this problem. One is to use the so-called “giant matrix” method [28], which consists of replacing the semi-infinite crystal with a giant slab containing a sufficiently large number of atom layers to reflect or absorb all incident electrons, and calculating the scattering within this slab in the spherical-wave representation (with great demand on computer storage and time). The other solution is to use the program CHANGE that was written by Jepsen<sup>6</sup> in the late 1960s, which we have used ever since. This program allows the user to bunch together two or more atomic layers, not only in the surface region (like other programs), but also throughout the bulk of the

TABLE I. Surfaces with interlayer spacing ( $d_{\text{bulk}}$ ) smaller than 1 Å studied by QLEED. The surfaces are listed in order of decreasing magnitude of  $d_{\text{bulk}}$ . The column headed "Calculation" specifies the computer program or procedure used: CHANGE is the program used in the present work, LD denotes layer doubling, GM denotes giant matrix, and RSMST denotes real-space multiple-scattering theory.

| Substrate                               | $d_{\text{bulk}}$ (Å) | Calculation | Reference    |
|---|-----------------------|-------------|--------------|
| Al{331}                                 | 0.926                 | LD          | 7            |
| Mo{111}                                 | 0.907                 | LD-GM       | 8            |
| Al{210}                                 | 0.906                 | LD          | 9            |
| Fe{310}                                 | 0.906                 | CHANGE      | 10           |
| Mo <sub>25</sub> Re <sub>75</sub> {111} | 0.903                 | LD-GM       | 11           |
| Pt{210}                                 | 0.877                 | RSMST       | 12           |
| NiAl{111}                               | 0.830                 | LD-GM       | 13           |
| Fe{111}                                 | 0.827                 | CHANGE      | 14           |
| Cu{211}                                 | 0.738                 | CHANGE      | 15           |
| Cu{511}                                 | 0.696                 | LD-GM       | 16           |
| Fe{210}                                 | 0.641                 | CHANGE      | 17           |
| Cu{320}                                 | 0.501                 | CHANGE      | Present work |
| Ag{410}                                 | 0.496                 | CHANGE      | 19           |

crystal, into composite layers, or "slabs," within which the multiple scattering is calculated in the angular momentum representation. Such a calculation has the disadvantage that it may scale in time approximately with the cube of the number of layers in the slab, since scattering between all pairs of atoms in the unit cell must be considered, but has the advantage that it allows very small interlayer distances, because it increases the regions in which the scattering is treated with spherical waves and decreases the regions in which the scattering is treated with plane waves.

To date, 13 surfaces with bulk interlayer spacings smaller than 1 Å have been studied with QLEED: we list them in Table I in order of decreasing  $d_{\text{bulk}}$ . The smallest  $d_{\text{bulk}}$  in this list is that of Ag{410}, but the analysis of that surface is somewhat uncertain, since it was based on a limited and very old database.<sup>18</sup>

The present paper is concerned with a QLEED analysis of a Cu{320} surface, for which  $d_{\text{bulk}}=0.501$  Å, with the CHANGE computer program. The compact step notation<sup>19</sup> for this surface is 3(110)(100), which tells that the surface features {110} terraces with three atom rows, separated by steps with normal in the <100> direction. If the rule requiring the periodicity of the oscillatory relaxation to be equal to the number of atoms in each terrace were valid for this surface, we would expect the sequence to be (- - + ...). But no theoretical study of this surface has been reported to date, as far as we know.

In Sec. II we present some experimental details and some characteristics of the experimental data from Cu{320}. In Sec. III we discuss the QLEED intensity analysis and give the results. In Sec. IV we summarize the conclusions.

## II. EXPERIMENT

A large single crystal of copper was aligned with X-ray Laue diffraction patterns for a cut perpendicular to a <320> direction. Two slices with a diamond saw produced a 2-mm-

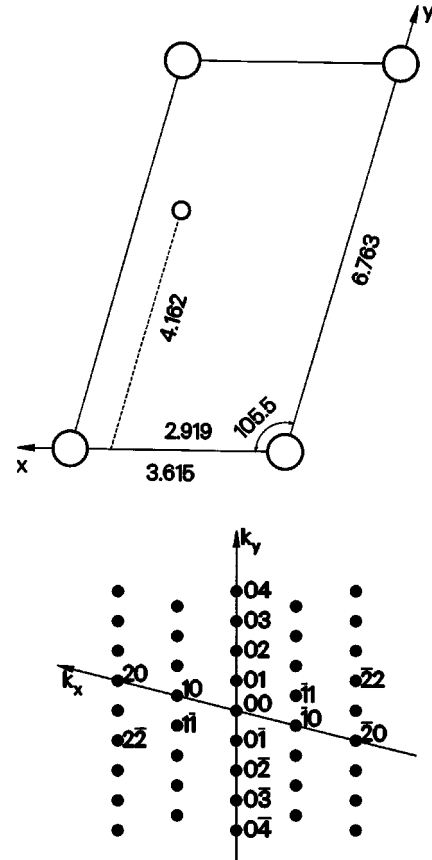


FIG. 1. Top: Unit mesh of Cu{320}: distances in Å, angle in degrees. The  $z$  axis points *into* the bulk: the interlayer spacing is  $d_{\text{bulk}}=0.501$  Å. Bottom: Schematic LEED pattern with representative indexing. The  $k_y$  axis is a mirror line.

thick platelet that was lapped and mechanically polished to within  $0.5^\circ$  of a {320} plane and finally electropolished to produce a mirrorlike surface. The platelet was then secured on a tantalum plate and mounted on a sample holder in an experimental chamber provided with a rear-view LEED system and a cylindrical mirror analyzer for AES (Auger electron spectroscopy) analysis.

After pumping, baking, and outgassing, the base pressure in the experimental chamber was routinely  $1 \times 10^{-10}$  Torr or lower. The sample surface was then cleaned with two argon bombardments of 5 h each ( $5 \times 10^{-5}$  Torr of Ar, 500 V, 2  $\mu$ A) and anneals (800–900 °C for 0.5 h) until the AES signals of C, S, and O (the only impurities present) were indistinguishable in the background noise of the analyzer.

The LEED pattern was the  $1 \times 1$  pattern expected from an fcc{320} surface, featuring only one mirror line, resulting from a bulk mirror plane perpendicular to the {320} surface. With the choice of unit mesh depicted in Fig. 1 (top), the mirror plane is perpendicular to the  $x$  axis, i.e., in reciprocal space, along the  $k_y$  axis, as drawn in Fig. 1 (bottom). This figure is a schematic representation of the LEED pattern, with some beam indices indicated. The mirror line produces normal-incidence degeneracies such as, e.g.,  $10 = \bar{1}1$ ,  $20 = \bar{2}2$ ,  $1\bar{1} = \bar{1}0$ , etc.

The orientation of the sample for normal incidence of the primary electron beam (orientation desired for the collection of diffracted intensity data) was helped in part, with respect

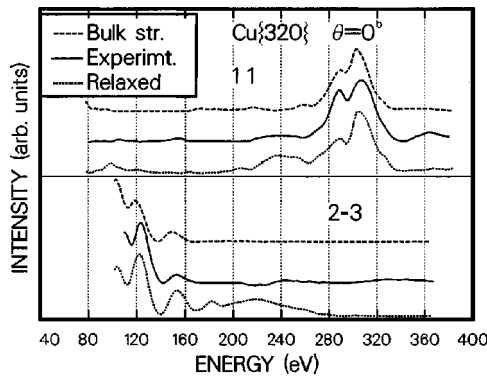


FIG. 2. Experimental (solid) and theoretical LEED  $I(V)$  spectra for  $\text{Cu}\{320\}$ . The upper curves in each panel (dashed) were calculated for a bulklike terminated surface; the bottom curves (dotted) represent the best fit to experiment found in the present work with the parameters given by the minimum of  $R_{\text{VHT}}$ .

to rotations around an axis parallel to  $k_y$ , by the presence of the mirror line: the sample was rotated around such an axis until all nominally degenerate beams had the same intensities. But no such help was available with respect to rotations around an axis perpendicular to  $k_y$ . Thus, to achieve normal incidence, we tried to use the method of Cunningham and Weinberg.<sup>20</sup> However, this method requires that the specular (or 00) beam be visible on the display screen of the LEED optics, i.e., that the sample be rotated *away* from normal incidence. We did so, determined the angle of incidence, and then rotated the sample *back* through the same angle. Unfortunately, the goniometer of our sample holder turned out to be insufficiently precise for this purpose. We kept the orientation found with this procedure, but we included the angle of incidence as an additional parameter to be determined in the course of the structure analysis, as described in the next section.

The intensities of several diffracted beams [the so-called  $I(V)$  curves or spectra] were then collected with a video-LEED system involving a television camera and a computer as described elsewhere.<sup>21</sup> The  $I(V)$  curves exhibit some characteristics that are worth noting (and are very probably typical for all stepped surfaces with bulk interlayer spacings of about 0.5 Å). The curves are predominantly kinematic, in the sense that they feature large peaks at or near the energies expected for kinematic (single-scattering) processes, and only weak to very weak intensity regions at intermediate energies, barely distinguishable from the background. These intensity regions (which we call “the grass” for short) contain most of the contributions from multiple-scattering processes and are therefore important, despite their weakness, for the quantitative analysis of the surface structure. The collection and the processing of intensity data were therefore in this case even more critical than usual: the signal-to-noise ratio was maximized with repeated signal-averaging measurements, and the subtraction of the background was done with particular care, in order to avoid losing important structural information.

A total of 43  $I(V)$  spectra were collected, of which 17 were pairwise degenerate and pairwise averaged, providing 26 nondegenerate curves (as depicted in Figs. 2–4) for the structure analysis. The total energy range amounts to  $\Delta E = 6110$  eV.

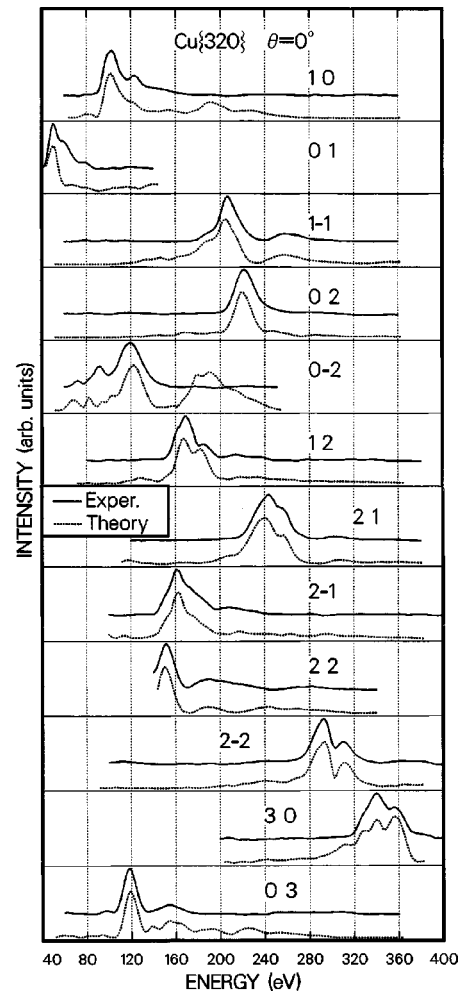


FIG. 3. Experimental (solid) and theoretical (dotted) LEED  $I(V)$  spectra for  $\text{Cu}\{320\}$ .

### III. ANALYSIS

The calculations of diffracted intensities were done with the CHANGE computer program<sup>6</sup> on a desktop personal computer (Pentium 300 MHz). The Cu potential was taken from the collection of Moruzzi, Janak, and Williams;<sup>22</sup> eight phase shifts were used, and the number of beams was changed in accordance with the electron energy (the maximum being 189 beams at 380 eV). The inner potential was put equal to  $-(10+4i)$  eV with the real part adjustable in the course of the analysis, and the root-mean-square amplitude of thermal vibrations was  $(\langle u^2 \rangle)^{1/2} = 0.15$  Å, corresponding to a Debye temperature  $\Theta_D = 304$  K.

With a bulk interlayer spacing of 0.5 Å, it was decided to treat the bulk of the crystal as composed of slabs including three atomic layers each (calculations bunching four layers in each slab did not produce significant differences in the spectra), and initially two, then three layers in the surface slab, thereby testing the first (12), the second (23), and the third (34) interlayer spacing.

As mentioned above, the unit mesh in real space was chosen as the rhombus depicted in Fig. 1 (top), with one edge of 3.615 Å along the  $x$  axis (pointing to the left) and the other of 6.763 Å along the  $y$  axis (pointing up). The angle between  $x$  and  $y$  is 105.5°, and the  $z$  axis points *into* the bulk of the crystal, with interlayer spacing  $d_{\text{bulk}} = 0.501$  Å.

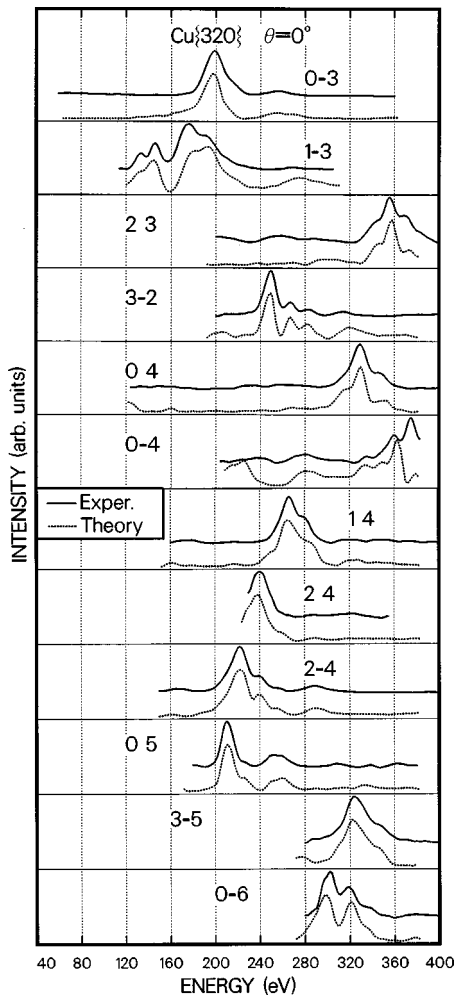


FIG. 4. Same as Fig. 3.

Before starting the search for the best structure parameters, it was necessary to find the azimuthal orientation of the sample during collection of experimental data, so that the calculations could be done for that same orientation (and the theoretical and experimental beam indices would then coincide). There are two possible orientations: one is as depicted in Fig. 1 (top), with the atom in the second layer at coordinates  $x=2.919 \text{ \AA}$  and  $y=4.162 \text{ \AA}$ ; the other with the sample (and the unit mesh) rotated azimuthally by  $180^\circ$ , i.e., with the unit-mesh origin diagonally opposite to that of the figure, and the  $x$  and  $y$  axes directed in opposite directions with respect to those drawn in the figure (in which case the second-layer atom would be at  $x=0.696 \text{ \AA}$  and  $y=2.601 \text{ \AA}$ ). The correct choice is easily made by making one calculation with, say, the first orientation, and then comparing calculated with experimental spectra. If, for example, the theoretical 10 curve agrees with the experimental 10 curve, then the chosen orientation is correct, otherwise the theoretical 10 curve will correspond to the experimental  $\bar{1}0$  curve, and the second orientation is correct (for this determination precise correspondence between calculated and experimental curves is not necessary, as usually 10 and  $\bar{1}0$  spectra are very different from one another).

In the search for the  $1 \times 1$  structure that fits the experimental curves best, normal incidence of the primary beam was assumed, and the first three interlayer spacings 12, 23,

and 34 were varied systematically, each time keeping two of them constant and varying the third one. We use the notation  $\Delta d_{12} = +0.10(-0.02)-0.18$  to indicate that the change  $\Delta d_{12}$  of the first interlayer spacing 12 was varied from  $+0.10 \text{ \AA}$  to  $-0.18 \text{ \AA}$  in steps of  $0.02 \text{ \AA}$ . After several tests with different parameter values, the refinement was done on a "grid search" including  $\Delta d_{12} = -0.08(-0.01)-0.18$ ,  $\Delta d_{23} = 0.0(-0.01)-0.17$ , and  $\Delta d_{34} = -0.1(0.025)+0.1$ .

The quality of fit between theory and experiment was judged both visually and by three  $R$  factors:  $R_{\text{VHT}}$ ,<sup>23</sup>  $r_{\text{ZJ}}$ ,<sup>24</sup> and  $R_p$ .<sup>25</sup> A characteristic of surfaces with small interlayer spacings is that even small changes in magnitude of the parameters constitute large percentage changes (e.g., a change of  $0.2 \text{ \AA}$  is a 40% change of a  $0.5\text{-\AA}$  interlayer spacing). A related observation is that, in contrast to surface structures with large interlayer distances (such as those of low-index surfaces), in the present case the values of all three  $R$  factors vary little for comparatively large percentage changes in the parameter values (e.g., changes in  $\Delta d_{12}$  of  $0.01 \text{ \AA}$  and  $\Delta d_{23}$  of  $0.02 \text{ \AA}$  changed  $r_{\text{ZJ}}$  from 0.0896 to 0.0880, and  $R_{\text{VHT}}$  from 0.2407 to 0.2368), and all  $R$ -factor minima were very shallow. It was therefore necessary to keep four significant figures after the period for all three  $R$  factors.

After optimization of the layer spacings with the assumed normal incidence had been achieved, the polar angle of incidence  $\theta$  was varied from  $0$  to  $0.2^\circ$  and  $0.4^\circ$ . For the azimuthal angle  $\phi$ , there were only two possible choices: the experimental situation was such that, if the incidence was not normal, the parallel component  $k_{\parallel}$  of the incident wave vector would lie along the  $k_y$  axis, so that the angle  $\phi$  could only be either  $+101.1^\circ$  or  $-78.9^\circ$  (for a precise definition of the angle  $\phi$ , see Ref. 26). The  $R$  factors were worsened in all cases, so that the normal-incidence assumption made for the calculations was proven correct.

With the best parameters found in the refinement, an attempt was made at testing the existence of possible parallel relaxation: in fact, a shift of atoms along the mirror plane is possible. Normal-incidence LEED is not very sensitive to in-plane atom shifts, but we nevertheless tried to displace the first-layer atoms by  $\pm 0.05$  and  $\pm 0.1 \text{ \AA}$  in the direction perpendicular to the  $x$  axis. No improvement of the  $R$  factors was obtained.

The  $R$ -factor minima (very shallow, as mentioned above) were as follows:  $R_{\text{VHT}}=0.2368$  for  $\Delta d_{12}=-0.12 \text{ \AA}$ ,  $\Delta d_{23}=-0.08 \text{ \AA}$ , and  $\Delta d_{34}=+0.05 \text{ \AA}$ ,  $r_{\text{ZJ}}=0.0880$  for  $\Delta d_{12}=-0.09 \text{ \AA}$ ,  $\Delta d_{23}=-0.14 \text{ \AA}$ , and  $\Delta d_{34}=+0.075 \text{ \AA}$ ,  $R_p=0.5383$  for  $\Delta d_{12}=-0.15 \text{ \AA}$ ,  $\Delta d_{23}=-0.03 \text{ \AA}$ , and  $\Delta d_{34}=+0.05 \text{ \AA}$ .

The minima of  $R_{\text{VHT}}$  and  $r_{\text{ZJ}}$  are indeed very low (especially considering the size of the experimental data set, with 26 nondegenerate beams over 6110 eV), but the minimum of  $R_p$  is disturbingly large. There is a reason for this result. The Pendry  $R$  factor is equally sensitive to very large and very small peaks in the  $I(V)$  curves (such as those in the "grass"). Unfortunately, very small peaks cannot be measured very accurately; hence it is natural that  $R_p$  would be large when a substantial portion of each  $I(V)$  spectrum has a lot of "grass," as is the case here and in general for high-index surfaces. In addition, the magnitude of  $R_p$  (whose definition is based on the logarithmic derivative  $L=I'/I$  of the intensity  $I$ ), can and usually does become unrealistically

large when  $I$  is very small. In fact, the magnitude of the  $R_P$  minimum is reduced by 45% to 0.24 if all the flat intensity regions are eliminated from the  $I(V)$  spectra (but then the data set becomes too small for a reliable analysis). The conclusion would appear to be, therefore, that the Pendry  $R$  factor is likely to be large when used with high-index surfaces, which have  $I(V)$  spectra with pronounced kinematic character, i.e., a single large peak (in the usually considered range from 40 to about 400 eV) and otherwise very low and flat intensity regions.

We quote the averages of the relaxations given by the three  $R$ -factor minima as the final result:

$$\Delta d_{12} = -0.12 \pm 0.03 \text{ \AA} \quad (\Delta d_{12}/d_{\text{bulk}} = -24 \pm 6)\%,$$

$$\Delta d_{23} = -0.08 \pm 0.06 \text{ \AA} \quad (\Delta d_{23}/d_{\text{bulk}} = -16 \pm 12)\%,$$

$$\Delta d_{34} = +0.06 \pm 0.03 \text{ \AA} \quad (\Delta d_{34}/d_{\text{bulk}} = +10 \pm 6)\%.$$

A characteristic of high-index surfaces is that the  $I(V)$  curves of the relaxed surface are very similar to those of the unrelaxed (bulklike) surface, although the  $R$  factors are different. In the present case the  $R$  factors for the unrelaxed surface are  $R_{\text{VHT}} = 0.3107$ ,  $r_{21} = 0.1675$ , and  $R_P = 0.6485$ , showing that the relaxed structure is a 31%, 90%, and 20% improvement, respectively, over the bulk-terminated structure. We show in Fig. 2, for two beams only, a comparison between experimental and corresponding calculated relaxed and unrelaxed curves. In Figs. 3 and 4 we show experimental and calculated curves for the remaining 24 beams: the calculated curves correspond to the structure chosen by  $R_{\text{VHT}}$  which is essentially the same as the structure with the final parameters listed above.

#### IV. CONCLUSION

The structure of a clean Cu{320} surface was found by quantitative low-energy electron diffraction to be relaxed with 24% contraction of the first layer, 16% contraction of the second, and 10% expansion of the third. Although no

calculation of the multilayer relaxation of Cu{320} has appeared in the literature, the interlayer relaxation sequence is expected to be  $(--+)$  and is herewith found experimentally.

The present work confirms the observation<sup>27</sup> that high-index (stepped) surfaces have  $I(V)$  spectra with pronounced kinematic character, involving the occurrence of only one (occasionally two) large intensity peak in the energy range usually considered in QLEED analyses (40 to about 400 eV), and otherwise long, mostly featureless low-intensity regions. This fact requires special care and precision in the collection of experimental intensity data, and particularly in the subtraction of the background. We believe that for this purpose the now obsolete method of collecting intensity data with a Faraday box (which measures electron currents directly and senses accurately small changes in small currents) would provide better data than the present method based on the fluorescence of phosphors in display-type LEED optics.

QLEED analyses of high-index surfaces generally reveal very shallow minima of the  $R$  factors, with the consequent need for four to five significant figures in the  $R$ -factor values. We have also noted that the low-intensity regions in the  $I(V)$  spectra make especially large contributions to the Pendry  $R$  factor, which can thereby become unrealistically high.

Finally, the present work confirms the usefulness and the power of the CHANGE computer program for QLEED analyses of surface structures with small interlayer spacings. The present case of Cu{320}, with bulk interlayer spacing of 0.501 Å, is one of two surfaces with the shortest interlayer spacing investigated by QLEED to date [the other is Ag{410} (Ref. 18) which, however, is somewhat uncertain owing to a limited experimental data set].

#### ACKNOWLEDGMENTS

We are very grateful to David Zehner and Gary Ownby for electropolishing the copper sample used in this work. We also gratefully acknowledge partial support from the National Science Foundation (NSF) with Grant No. DMR9806651.

- <sup>1</sup>B. Loisel, D. Gorse, V. Pontikis, and J. Lapujoulade, *Surf. Sci.* **221**, 365 (1989).
- <sup>2</sup>P. A. Gravil and S. Holloway, *Phys. Rev. B* **53**, 11 128 (1996).
- <sup>3</sup>S. Durukanuđlu, A. Kara, and T. S. Rahman, *Phys. Rev. B* **55**, 13 894 (1987).
- <sup>4</sup>C. Wei, S. P. Lewsi, E. J. Mele, and A. M. Rappe, *Phys. Rev. B* **57**, 10 062 (1998).
- <sup>5</sup>I. Yu. Sklyadneva, G. G. Rusina, and E. V. Chulkov, *Surf. Sci.* **416**, 17 (1998).
- <sup>6</sup>D. W. Jepsen, *Phys. Rev. B* **22**, 5701 (1980); **22**, 814 (1980).
- <sup>7</sup>D. L. Adams and C. S. Sørensen, *Surf. Sci.* **166**, 495 (1986).
- <sup>8</sup>M. Arnold, A. Fahmi, W. Frie, L. Hammer, and K. Heinz, *J. Phys.: Condens. Matter* **11**, 1873 (1999).
- <sup>9</sup>D. L. Adams, V. Jensen, X. F. Sun, and J. H. Vollesen, *Phys. Rev. B* **38**, 7913 (1988).
- <sup>10</sup>J. Sokolov, F. Jona, and P. M. Marcus, *Phys. Rev. B* **29**, 5402 (1984).
- <sup>11</sup>L. Hammer, M. Kottcke, M. Taubmann, S. Meyer, C. Rath, and

- K. Heinz, *Surf. Sci.* **431**, 220 (1999).
- <sup>12</sup>X.-G. Zhang, M. A. Van Hove, G. A. Somorjai, P. J. Rous, D. Tobin, A. Gonis, J. M. MacLaren, K. Heinz, M. Michl, H. Lindner, K. Müller, M. Ehsasi, and J. H. Block, *Phys. Rev. Lett.* **67**, 1298 (1991).
- <sup>13</sup>J. R. Noonan and H. L. Davis, *Phys. Rev. Lett.* **59**, 1714 (1987).
- <sup>14</sup>J. Sokolov, F. Jona, and P. M. Marcus, *Phys. Rev. B* **33**, 1397 (1986).
- <sup>15</sup>Th. Seyller, R. D. Diehl, and F. Jona, *J. Vac. Sci. Technol. A* **17**, 1635 (1999).
- <sup>16</sup>M. Albrecht, R. Blome, H. L. Meyerheim, W. Moritz, and I. K. Robinson, *Surf. Sci.* (to be published).
- <sup>17</sup>J. Sokolov, F. Jona, and P. M. Marcus, *Phys. Rev. B* **31**, 1929 (1985).
- <sup>18</sup>F. Jona, E. Zanazzi, M. Maglietta, and P. M. Marcus, *Surf. Rev. Lett.* **6**, 355 (1999).
- <sup>19</sup>B. Lang, R. W. Joyner, and G. A. Somorjai, *Surf. Sci.* **30**, 454 (1972).

- <sup>20</sup>S. L. Cunningham and W. H. Weinberg, *Rev. Sci. Instrum.* **49**, 7 (1978).
- <sup>21</sup>F. Jona, J. A. Strozier, Jr., and P. M. Marcus, in *The Structure of Surfaces*, edited by M. A. Van Hove and S. Y. Tong (Springer-Verlag, Berlin, 1985), p. 92.
- <sup>22</sup>V. L. Moruzzi, J. F. Janak, and A. R. Williams, *Calculated Electronic Properties of Metals* (Pergamon, New York, 1978).
- <sup>23</sup>M. A. Van Hove, S. Y. Tong, and M. H. Elconin, *Surf. Sci.* **64**, 85 (1977); M. L. Xu and S. Y. Tong, *Phys. Rev. B* **31**, 6332 (1985).
- <sup>24</sup>E. Zanazzi and F. Jona, *Surf. Sci.* **62**, 61 (1977).
- <sup>25</sup>J. B. Pendry, *J. Phys. C* **13**, 937 (1980).
- <sup>26</sup>F. Jona, *J. Phys. C* **11**, 4271 (1978).
- <sup>27</sup>F. Jona, *Surf. Rev. Lett.* (to be published).
- <sup>28</sup>M. A. Van Hove, W. H. Weinberg, and C.-M. Chan, *Low-Energy Electron Diffraction* (Springer, New York, 1986), p. 158.